Molecular Design of Two-dimensional Perovskite Cations for Efficient Energy Cascade in Perovskite Light Emitting Diodes

Nur Fadilah Jamaludin[a], Benny Febriansyah[a], Yan Fong Ng[a], Natalia Yantara[a], Mingjie Li[c], David Giovanni[c], Jianhui Fu[c], Yeow Boon Tay[a], Tom Baikie[a], Tze Chien Sum[c], Nripan Mathews[a, b*], Subodh Mhaisalkar[a, b]

[a] *Energy Research Institute @ NTU, Nanyang Technological University, Research Techno Plaza, X-Frontier Block, Level 5, 50 Nanyang Drive, 637553, Singapore*

[b] *School of Materials Science and Engineering, Nanyang Technological University, 50 Nanyang Avenue, 639798, Singapore*

[c] *Division of Physics and Applied Physics, School of Physical and Mathematical Sciences, Nanyang Technological University, 21 Nanyang Link, 637371, Singapore*

[*] *Author to whom correspondence should be addressed. Email: nripan@ntu.edu.sg*

Despite extensive reports on highly efficient perovskite light-emitting diodes (PeLEDs), rules governing design of suitable two-dimensional (2D) perovskite templating cation to facilitate formation of optimal emitter landscape for energy cascade, remain largely elusive. With factors such as structure, size, functionalization and charge, capable of influencing the distribution of multidimensional perovskite phases, the importance of 2D templating cation design in determining film optoelectronic properties is indisputable. However, typical mono-functionalized 2D templating cations often result in larger lead halide octahedral spacing, which impedes effective charge transport. This has fueled investigation into the use of multiple cations for optimal domain distribution and improved charge transfer kinetics to the emitting species. In this study, we attempt to impart enhanced charge transfer characteristics to the resultant multidimensional perovskite by employing two bi-functionalized aromatic cations, namely pyridinium ethyl ammonium (PyrEA) and imidazolium ethyl ammonium (ImEA), reminiscent of mono-functionalized phenyl ethyl ammonium (PEA), a widely used 2D perovskite templating cation. Although it is proposed that the greater intermolecular bonding would enhance charge transfer rates, the simultaneous increase in lead halide octahedral distortion results in quenching of their corresponding 2D and multidimensional perovskite luminescence properties, correlated with increased defect density within the material. This manifests in the form of shorter PL decay lifetimes, lower PLQY, and device performance arising from inferior energy funneling. This study highlights the importance of designing 2D perovskite templating cations offering better transport and reduced octahedral distortion for the development of energy cascade-efficient, multidimensional perovskites.

Perovskite-based light-emitting diodes (PeLEDs) have shown steep performance trajectory owing to its novel semiconducting properties such as low defect densities and strong photoluminescence (PL) characteristics,[1-3] as well as the extensive knowledge gained from their deployment as light absorbers. However the inherent limitations of three-dimensional (3D) lead halide perovskites ($APbX_3$, where A is represented by Cs, CH_3NH_3 or $CH(NH_2)_2$ while X is either Cl, Br or I) in terms of low exciton binding energy, moisture and light instability, impede development of high efficiency PeLEDs.[4-6] This has driven research into two-dimensional (2D) perovskites, which apart from their superior ambient stability, offer high exciton binding energies, thereby increasing their attractiveness for light emission applications.[1]Depending on the type of 2D cation employed, mixing both the 2D and 3D species would yield either Ruddlesden-Popper ($L_2A_{n-1}Pb_nX_{3n+1}$) or Dion-Jacobson ($L'A_{n-1}Pb_nX_{3n+1}$) perovskites, with L and L' referring to mono- and bi-functionalized bulky organic molecular cation whereas *n* corresponds to the number of PbX_6^{4-} layers present. As a result, the energetic emitter landscape, made up of numerous domains of varying bandgaps, transforms in electronic structure to one reminiscent of a multi quantum well.[7] During device operation, injected charge carriers, aided by the energetic emitter landscape, funnel from higher to lower bandgap domains before recombining radiatively.[8-10] Due to the rapid time scales at which the charge transfer phenomenon occurs, non-radiative recombination in the high bandgap domains is effectively suppressed, promoting higher radiative recombination. While the recombination regime (monomolecular or bimolecular) may differ depending on the resultant film composition[11], higher performance is still achieved at lower voltages in these systems due to superseding of non-radiative recombination events.[10, 12] In addition, the ease of spectral tuning via variation of 2D and 3D cation ratio presents the energy cascade concept an attractive approach for efficient light emission.[9, 13, 14]

Despite numerous reports on multidimensional perovskites for light emission,[7, 13, 15] knowledge on the type of 2D perovskite templating cation required to facilitate formation of optimal emitter landscape for energy cascade, remains unclear. Depending on the cation structure, size, charge, and position of the functional group employed, the resulting lead halide octahedral can be altered, highlighting the importance

of organic cation selection in determining the resultant multidimensional perovskite properties. For example, utilizing bi-functionalized cation enables the distance between the inorganic layers to be reduced, hence giving rise to enhanced charge transport[16], reduced excitonic binding energy[17] and smaller bandgap as compared to their mono-functionalized organic cation counterpart.[18] The position of the functional group also changes the cation flexibility resulting in varying degrees of lead octahedral packing. Knutson, Martin, and Mitzi as well as Kamminga, de Wijs, Havenith, *et al.* have shown that the bandgap of the 2D iodide perovskites can be tuned by structural distortion and connectivity of the metal halide octahedra due to their influence on the electronic structure.[19, 20] Bi-functionalized ligands have not only been employed to mitigate surface defects [21] but may also improve coupling between the various multidimensional phases for enhanced charge transfer[22, 23]. Hence, understanding the influence of 2D perovskite templating cation on 2D and multidimensional perovskites, is crucial for their successful deployment in optoelectronics. Especially for light emission where the dependency of photo- and electroluminescence efficiencies on radiative and non-radiative recombination processes as well as charge transfer kinetics, underscores the importance of assessing templating cation structural effect for high performance PeLEDs.

Here, the impact of 2D perovskite templating cation design on the resulting perovskite properties, particularly the charge transfer kinetics, will be assessed by employing two bi-functionalized aromatic cations, namely pyridinium ethyl ammonium (PyrEA) and imidazolium ethyl ammonium (ImEA) (**Figure 1a**). Reminiscent of phenyl ethyl ammonium (PEA), a widely used mono-functionalized 2D perovskite templating cation, it was proposed that the dual bonding offered by PyrEA and ImEA would impart enhanced charge transfer characteristics in the resultant multidimensional perovskite, potentially enabling higher PeLED efficiencies to be attained. However, in spite of the additional intermolecular interaction, the simultaneous increase in octahedral distortion following the substitution of PEA with ImEA and PyrEA, leads to poorer PL and device properties, highlighting the need for a more holistic approach towards the design of suitable 2D templating cation. This would ensure that desired charge transfer

capabilities be achieved without detriment to other film properties. To provide for a more comprehensive understanding of the influence 2D perovskite templating cation design has on resultant multidimensional perovskite properties, investigation into the pure 2D perovskites was first initiated.

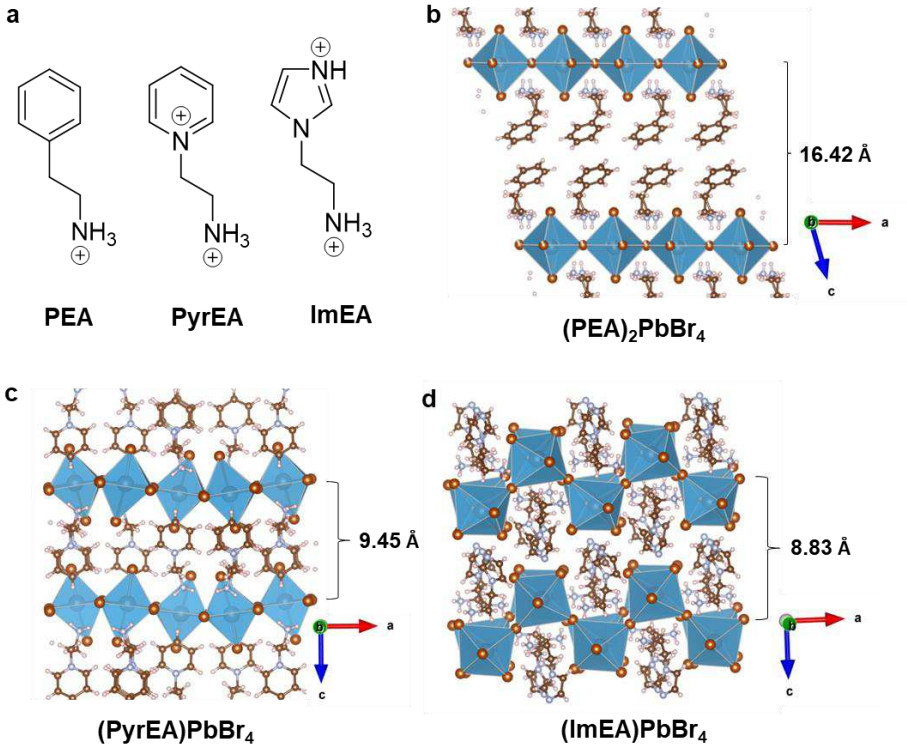

Figure 1 (a) Molecular structures of PEA, PyrEA and ImEA cations as well as crystal structures of pure (b) $(PEA)_2PbBr_4$, (c) $(PyrEA)PbBr_4$ and (d) $(ImEA)PbBr_4$ 2D perovskites.

Single crystals of $(PEA)_2PbBr_4$, $(PyrEA)PbBr_4$ and $(ImEA)PbBr_4$ are first grown through a process as described in **Supplementary Note 1**. Single-crystal X-ray diffraction (XRD) analysis indicates that both $(PEA)_2PbBr_4$ and $(PyrEA)PbBr_4$ possess <001> oriented perovskite structures (**Figure 1b- c**). A smaller spacing between the inorganic octahedral layers for $(PyrEA)PbBr_4$ and $(ImEA)PbBr_4$ as compared to $(PEA)_2PbBr_4$ is expected as the divalent nature of PyrEA and ImEA promotes the formation of a single

organic layer between the lead halide octahedra layers. On the other hand, the binding of ImEA monolayer to the two inorganic layers in the corresponding 2D structure results in a <110> oriented perovskite lattice arrangement (**Figure 1d**). The corrugated structure of (ImEA)$PbBr_4$ arises from the hydrogen bonding interaction between the N-H functional group of the imidazole core and the neighboring bridging bromide ions of the inorganic layers.[16] Here, it is evident that the molecular design of the 2D perovskite templating cation plays a direct role in influencing the lead halide octahedra packing, with dual bonding resulting in the narrowing of interlayer spacing.

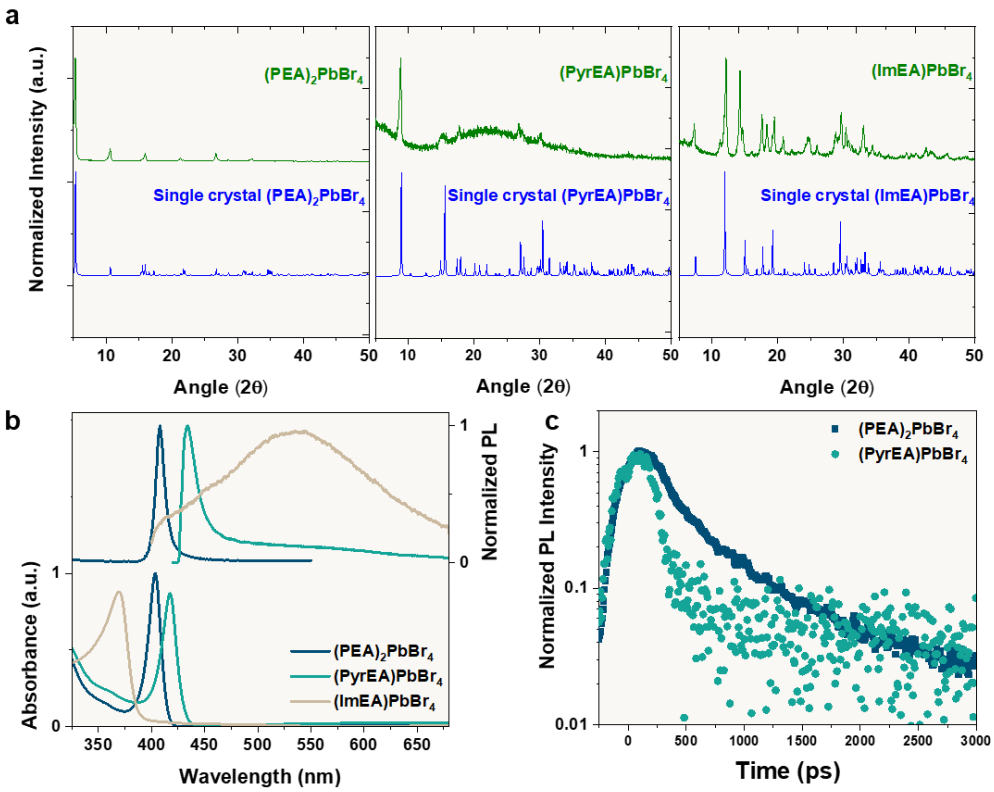

Figure 2 (a) Single-crystal and thin film XRD patterns of pure 2D $(PEA)_2PbBr_4$, (PyrEA)$PbBr_4$ and (ImEA)$PbBr_4$, (b) Absorbance and steady-state PL spectra of $(PEA)_2PbBr_4$ as well as (PyrEA)$PbBr_4$ and (ImEA)$PbBr_4$. (c) Transient PL decays of $(PEA)_2PbBr_4$ and (PyrEA)$PbBr_4$ films.

As the processing condition is known to influence the formation and thus optoelectronic properties of perovskite films, XRD patterns of spincoated $(PEA)_2PbBr_4$, (PyrEA)$PbBr_4$ and (ImEA)$PbBr_4$ films prepared from stoichiometric ratios of their precursor materials, are obtained to verify the formation of pure 2D perovskites (**Figure 2a**). It is revealed that the fabricated films are phase pure with characteristic peaks corresponding to the respective 2D perovskite phases. This affirms the 2D perovskite templating capability of PyrEA and ImEA via solution-based processing. The $(PEA)_2PbBr_4$ sample exhibits more

regularly spaced diffraction peaks as compared to both (PyrEA)$PbBr_4$ and (ImEA)$PbBr_4$ samples, accrued to its more symmetric structure (**Figure 1b**). The optical properties of the 2D perovskite materials are subsequently characterized to assess the impact of templating cation design (**Figure 2b**). From the absorption spectra, only a single excitonic absorbance feature is observed. A bathochromic shift is observed in (PyrEA)$PbBr_4$ relative to $(PEA)_2PbBr_4$, while $(ImEA)_2PbBr_4$ exhibits the most blue-shifted excitonic transition between the two. The former is attributed to the Pb–(μ-Br)–Pb bond angles approaching ideal values, (180°; see **Table S1**) stabilizing the conduction band and narrowing their bandgaps[24, 25], while the latter is due to poorer Pb 6s and Br 4p orbital overlap in the corrugated sheets relative to (100) oriented structures[26, 27]. Similarly, PL spectra of the three films differ. Although both $(PEA)_2PbBr_4$ and (PyrEA)$PbBr_4$ exhibit narrow emission line-widths, (ImEA)$PbBr_4$, on the other hand, gives a broad emission peak extending from ~ 400 to 700 nm, likely stemming from self-trapped excitons.[28, 29] The PL broadening, particularly for (ImEA)$PbBr_4$, arises from the increased structural distortion,[30] manifesting in low PL despite the high exciton binding energies up to hundreds of meV typical of 2D perovskites.[31] To further verify this, transient PL decay of the 2D perovskite thin films was carried out to investigate the photoexcited charge dynamics (**Figure 2c**), where $(PEA)_2PbBr_4$ and (PyrEA)$PbBr_4$ exhibit average lifetimes of 473 and 143 ps respectively whereas the poor PL characteristic of (ImEA)$PbBr_4$ resulted in the absence of measurable PL decay. The poor PL properties and short lifetimes indicate that the highest non-radiative recombination losses occur in (ImEA)$PbBr_4$, followed by (PyrEA)$PbBr_4$ and $(PEA)_2PbBr_4$. It is hypothesized that non-radiative recombination in 2D perovskites is proportional to the degree of lead octahedra distortion, which increases on substitution of PEA with PyrEA and ImEA. A quantitative distortion parameter, the lead halide octahedral distortion (Δd) is obtained by assessing the layered framework structure, comprising of quadratic elongation of the metal-halide bond (λ_{oct}), and bond angle variance of the halide-metal-halide (Br-Pb-Br) angle (σ_{oct}^2) (**Supplementary Note 2**). For a crystal structure to exhibit minimal octahedral distortion, the following criteria need to be fulfilled: (a) low Δd value, (b) λ_{oct} approaching 1, and (c) low σ_{oct}^2.[30, 32, 33] Based on the criteria

mentioned above, it can be deduced that $(PEA)_2PbBr_4$ yields the lowest degree of distortion followed by $(PyrEA)PbBr_4$ and $(ImEA)PbBr_4$ **(Table 1)**. The relatively larger octahedral distortion in $(PyrEA)PbBr_4$ and $(ImEA)PbBr_4$ is attributed to the inherently asymmetric environment of their constituent $[PbBr_6]^{4-}$ octahedra, which is absent in the case of $(PEA)_2PbBr_4$. In particular, the bi-functionalized organics within the monolayer alternate in terms of their orientation, with either their aromatic heads or ethylammonium tails pointing into the "bay regions" formed by the axial bromide ions of four nearest neighbouring Pb-Br octahedra. Additionally, the two "bay regions" on opposing faces of the 2D inorganic sheets host different ends (heads or tails) of the bi-functionalized cations. Such asymmetry is further exacerbated by the large difference between penetration of the heads and tails of the bi-functionalized cations into the "bay regions" of the perovskites.

Table 1 Summary of Δd, λ_{oct} and σ_{oct}^2 of pure 2D $(PEA)_2PbBr_4$, $(PyrEA)PbBr_4$ and $(ImEA)PbBr_4$ obtained from single-crystal XRD analysis.

Compound	Octahedral Distortion		
	Δd (10^{-4})	λ_{oct}	σ_{oct}^2
$(ImEA)PbBr_4$	22.93	1.0177	53.67
$(PyrEA)PbBr_4$	19.59	1.0131	36.41
$(PEA)_2PbBr_4$	10.89	1.0056	15.70

Moreover, the formation of multiple photoinduced emissive colour centres in these films, induced by larger deformation of the Pb–Br bond length and Br–Pb–Br bond angles in the inorganic lattices lead to more defective electronic structures[30, 34]. As such, we deduce that a 2D cation molecular design promoting the formation of perovskite crystals with a lower degree of lead halide octahedra distortion is key to achieving better luminescence properties of 2D perovskites.

Next, the 2D cations are added in excess to 3D $FAPbBr_3$ precursors, with the ratio of 2D:3D cations (2:5) kept the same across all prepared solutions to assess effect of 2D cation molecular design on resultant

multidimensional perovskites. The XRD patterns of these films (**Figure S1**) confirm that phase segregation did not occur as noted by the absence of characteristic 2D perovskite peaks at low 2θ angles (below 10°). Instead, the peaks from the 2D-3D films are mainly assigned to the 3D $FAPbBr_3$ perovskite. Generally, across the three 2D-3D perovskite films, two observations can be made from the XRD analysis; (a) reduction in reflection intensities, which is attributed to reduced crystallinity and (b) the presence of new peaks at higher 2θ angles (beyond 29°), relative to the 3D, possibly due to increased strain or a change in crystal symmetry.

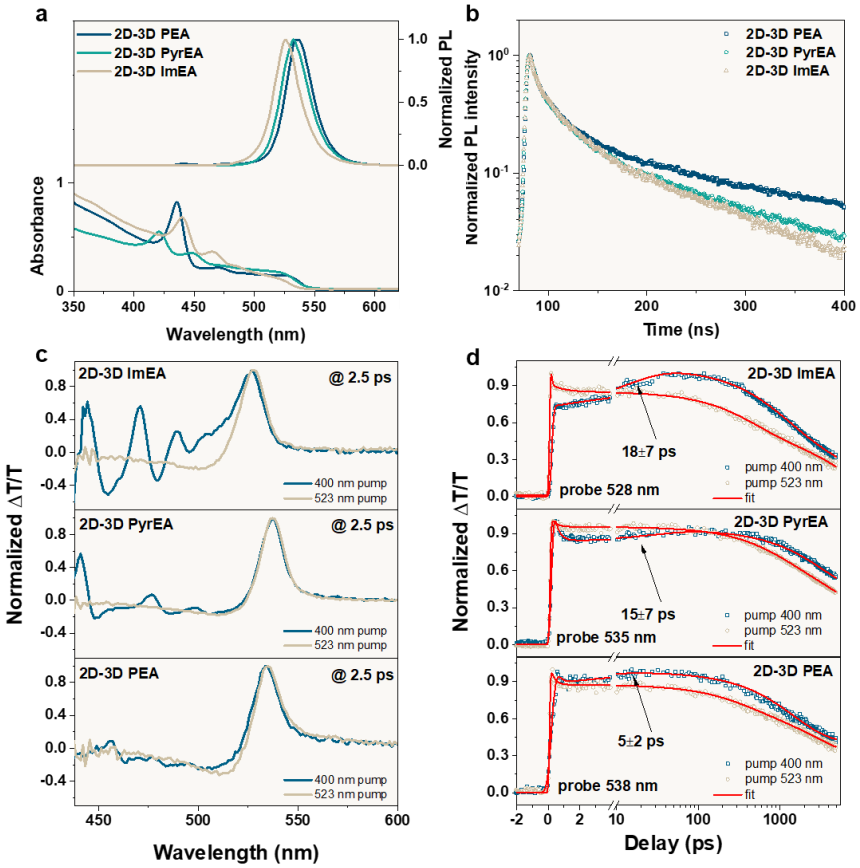

Figure 3 (a) Absorbance and normalized PL spectra, (b) transient PL decay lifetimes (λ_{exc} = 405 nm), and transient absorption spectra depicting the charge transfer kinetics (measured using 400 nm (dark blue) and

523 nm (grey) laser excitation, and probed at the band-edge photobleaching peaks) plotted as (c) a function of delay time and (d) wavelength for 2D-3D PEA, 2D-3D PyrEA and 2D-3D ImEA.

The absence of excitonic absorbance peaks around 405 nm, 417 nm and 370 nm for the 2D-3D PEA, 2D-3D PyrEA and 2D-3D ImEA films, respectively (**Figure 3a**) concur with the XRD data, which indicate the absence of pure 2D domains. On the other hand, the dual peaks observed at 435 and 470 nm for 2D-3D PEA, 420 and 450 nm for 2D-3D PyrEA as well as 440 and 465 nm for 2D-3D ImEA suggest the formation of lower dimensional domains (n = 2, 3, 4…). The formation of different domains in the 2D-3D perovskite films could also provide explanation for the emergence of additional peaks in the higher 2θ angle regions of the XRD patterns (**Figure S1**). The absorption edge of the three films are similar and fall within the expectation of pure 3D domains. On excitation of the 2D-3D films with a 405 nm laser, the films exhibited PL emissions ~ 535 nm (**Figure 3a**), corresponding to that from the 3D domains. Although 2D (ImEA)$PbBr_4$ exhibits broad emission which spans the 3D emission range, the primary emission of its corresponding 2D-3D perovskite is assigned to the 3D perovskite owing to the significantly narrower emission line-width. Quasi-2D emission peaks are expected in the region below 500 nm due to the correlation to excitonic absorbance features of the three 2D-3D films. For clarity, the PL spectra is presented in logarithmic scale (**Figure S2**) to enable better visualization of the lower-dimensional domain emissions. While two additional quasi-2D emission features are detected for 2D-3D PEA (440 and 475 nm), barely any peaks are observed for 2D-3D ImEA and 2D-3D PyrEA, possibly due to the weakly-emitting nature of these lower dimensional domains. The photoluminescence quantum yield (PLQY) of the three films are subsequently measured with 2D-3D PEA revealed to have the highest PLQY of 35%, while 2D-3D PyrEA and 2D-3D ImEA show significantly lower values of 18% and 15% respectively. Transient PL spectroscopy is also measured at the primary emission wavelengths (**Figure 3b**). The decay lifetimes are fitted with a bi-exponential decay function yielding average decay lifetimes of 32.1, 27.7 and 19.3 ns for 2D-3D PEA, 2D-3D PyrEA and 2D-3D ImEA films respectively. The higher PLQY, longer PL lifetime and shorter radiative lifetime (**Table S2**) of 2D-3D PEA, provide evidence of its lower non-

radiative recombination losses as compared to 2D-3D PyrEA and 2D-3D ImEA. This suggests that the distinct electronic defectivity observed in the pure 2D perovskites optical properties arising from increased Pb-Br octahedral distortion, also translates to the corresponding 2D-3D films.

Typically, high PL intensity particularly at low excitation power is desired, reflective of low radiative recombination losses and high radiative recombination efficiency. On comparing the PL intensity of the three 2D-3D films at primary emission wavelength across different pump fluences (**Figure S3**), unsurprisingly, 2D-3D PEA yields the highest PL intensity, further confirming its radiative recombination efficiency. The highly localized charge carrier concentration in the emitting domains, facilitated by the energy funneling process, promotes high radiative recombination, leading to the higher PL intensities observed in these systems relative to 3D perovskites.[13, 35] This provides basis for the higher PL intensities shown by 2D-3D PEA. The trend in the PLQY values for these multidimensional systems are likely due to three reasons; (a) the prevalence of defects, (b) the efficiency of radiative recombination occurring in the lowest bandgap domains and (c) the efficacy of charge carrier funneling between the high bandgap and low bandgap phases. Based on the characterization of both the 2D single crystals as well as 2D-3D thin films, it is clear that the 2D cation design is crucial not only for the templating of low defect density multidimensional perovskites, but also for an optimal phase distribution to promote high radiative recombination. It is well-reported that high defect densities in perovskite promotes non-radiative recombination losses, thereby suppressing the advantage offered by the energy cascade process [4, 36, 37]. With less charge carriers effectively transferred from the higher bandgap domains to the smallest bandgap emitting domains, the lower eventual concentration of charge carriers in the emitting domains results in less radiative recombination. Charge carrier funneling efficacy is just as important for efficient PeLEDs as it is for high PLQY. This is due to the increase in undesired Auger recombination with higher charge carrier densities, which may occur due to buildup of charge carriers in non-emitting domains [5].

To correlate the 2D perovskite templating cation structure with charge transfer or energy funneling efficacy of the corresponding 2D-3D films, transient absorption spectroscopy studies are carried out.

Unlike 2D-3D PyrEA and 2D-3D ImEA, where several photobleaching peaks corresponding to carrier filling are observed, only two peaks are noted for 2D-3D PEA (**Figure 3c**). This can be accrued to the high carrier funneling efficiency afforded by using PEA as a templating cation. The dynamics of photobleaching for these 2D-3D films pumped at 400 and 523 nm and probed at the band-edge pbotobleaching peaks (i.e., $n = \infty$), further confirm the extremely short funneling time of 2D-3D PEA (around 5 ps) as compared to around 15 and 18 ps for 2D-3D PyrEA and 2D-3D ImEA respectively (**Figure 3d**). Moreover, PL excitation spectra (**Figure S4**) reveal a significantly greater increase in PL intensity upon excitation of lower dimensional phases for 2D-3D PEA than 2D-3D PyrEA and 2D-3D ImEA, implying significantly greater influence of the lower dimensional domains in enhancing the primary emission for 2D-3D PEA. The smaller change in PL intensity when the 2D-3D PyrEA and 2D-3D ImEA films are excited at these wavelengths is attributed to the more defective nature of these films. The higher charge funneling efficiency and enhanced emission on excitation of lower dimensional phases of 2D-3D PEA are in strong agreement with improved optical properties of less defective systems. Thus, prudent choice of 2D perovskite templating cation exhibiting low lead octahedral distortion is necessary to promote efficient energy funneling for high PLQY. Morphological studies of these films reveal similar surface topologies for 2D-3D PEA and 2D-3D ImEA (**Figure S5**), where smooth compact films are formed on spin coating the films. However, in the case of 2D-3D PyrEA, a rougher film, consisting of distinct grooves demarcating the individual large grains, is observed through cross-sectional imaging.

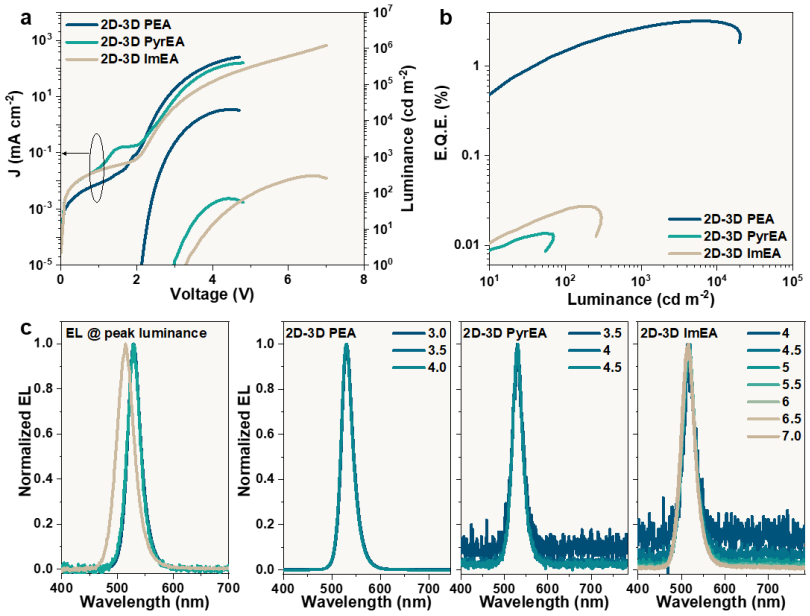

Figure 4 (a) Current density (J) and luminance against voltage curves, (b) EQE against luminance, (c) normalized EL spectra of each 2D-3D PeLED at peak luminance, and (d) normalized EL spectra at various voltage application for 2D-3D PEA (left), 2D-3D PyrEA (middle) and 2D-3D ImEA (right).

To assess the performance of these films from a device perspective, PeLEDs with an ITO/PEDOT:PSS/2D-3D perovskite/PO-T2T/LiF/Al (**Figure S6**) configuration, are subsequently fabricated (**Figure 4**). Based on the device characteristics, 2D-3D PEA yields the best performance, where lower threshold voltage (V_{th} (voltage at 1 cd.m^{-2}) = 2.2 V), higher luminance (L_{max} > 20 k cd m^{-2}), and external quantum efficiency (EQE = 3%) are noted compared to those for 2D-3D PyrEA and 2D-3D ImEA (**Figure 4a-b**). The low V_{th} of 2D-3D PEA implies a low charge carrier injection barrier and effective radiative recombination, supported by the low current density required for high luminance (**Figure 4a**). The steep increase in the luminance on device turn on indicates rapid radiative recombination process occurring during device operation as explained by the efficient energy funneling process. Despite the low

current density, the rapid energy transfer process coupled with low defect density and high radiative recombination efficiency ensure that losses due to non-radiative recombination, are minimized. In comparison, the 2D-3D PyrEA and 2D-3D ImEA devices require higher operating voltages and exhibit higher leakage current, which suggest that the injected carriers are not effectively confined for radiative recombination despite the energetic emitter landscape. This means that the carriers are likely to be lost to other non-radiative processes in the more distorted structures of these systems, which then manifest in the form of 2 orders of magnitude lower luminance and efficiencies. Moreover, the difference in energetics of the 2D-3D perovskite and its adjacent layers, provides an added explanation for the disparity in performance of the 2D-3D films. The band alignment for 2D-3D PEA promotes reduced barrier for charge carrier injection as opposed to 2D-3D PyrEA and 2D-3D ImEA, translating in the higher V_{th} noted for the latter devices. The EL peak at L_{max} (**Figure 4c**) concur with the PL spectra, where both 2D-3D PEA and 2D-3D PyrEA exhibit similar emission with slight blue shifting of emission observed for 2D-3D ImEA. Despite the dramatic difference in device performance for 2D-3D PEA, 2D-3D PyrEA and 2D-3D ImEA, the peak EL wavelengths remain unchanged throughout the duration of measurement (**Figure 4d**), indicating optimal ratio of donor to acceptor phases in these films, thus ensuring monochromatic emission[9, 38]. In comparison, pristine 3D $FAPbBr_3$ device shows poorer device performance (**Figure S7**) than the devices adopting the energy funneling concept. This is due to the enhanced charge confinement and radiative recombination process afforded by the multi quantum well structure in the 2D-3D perovskites, further highlighting the importance of the energy funneling process and the selection of suitable 2D templating cation for development of highly efficient PeLEDs.

In summary, although the use of bi-functionalized cations such as PyrEA and ImEA offer the possibility of enhancing charge transfer between various multidimensional perovskite phases, the increase in lead bromide octahedral distortion in their perovskite inorganic lattices and its influence over luminescence properties of both pure 2D and multidimensional perovskites, suggest the need to consider octahedral distortion as a criterion in rational 2D perovskite templating cation design. Depending on the cation

charge, size, and location of its functional group, the orientation of the resulting 2D perovskite could be altered from <001> to <110>, as seen in the case of (ImEA)$PbBr_4$. In general, molecules that generate 2D perovskite with a greater degree of octahedral distortion (ImEA > PyrEA > PEA) are associated with poorer luminescence properties because of high non-radiative recombination losses from the more defective structures. When mixed with $FAPbBr_3$ to form multidimensional perovskites, the films based on the 2D cation molecules which promote a higher degree of octahedral distortion similarly exhibit lower PLQY values and shorter PL decay lifetime. In these multidimensional systems, the energy funneling process is further affected by more distorted structures leading to additional shunt pathways, which greatly reduce the population of funneled charge carriers (or energy) in the lowest bandgap domains. This consequently results in 2D-3D PEA PeLED achieving 2 orders of magnitude higher luminance and efficiency as compared to the 2D-3D ImEA and 2D-3D PyrEA devices. Design of more efficient multidimensional PeLEDs will thus require screening of 2D cation molecules that promote lower octahedral distortion while offering good charge transport properties in order to achieve an effective energy funneling process with minimal non-radiative losses.

Supplementary Information
See supplementary information for more details on experimental procedures and other information.

Data Availability Statement
The data that supports the findings of this study are available within the article [and its supplementary material].

Acknowledgements

This research was primarily supported by the National Research Foundation under its Competitive Research Programme (CRP Award No. NRF-CRP14-2014-03) and the Ministry of Education under MOE2018-T2-2-083. The photophysical measurements are supported by National Research Foundation Investigatorship (NRF-NRFI-2018-04) and by the Ministry of Education under MOE Tier 2 grant MOE-T2EP50120-0004.

[1] S. A. Veldhuis, P. P. Boix, N. Yantara *et al.*, "Perovskite Materials for Light-Emitting Diodes and Lasers," *Advanced Materials,* pp. 6804-6834, 2016, doi: 10.1002/adma.201600669.

[2] L. Xu, S. Yuan, H. Zeng *et al.*, "A comprehensive review of doping in perovskite nanocrystals/quantum dots: evolution of structure, electronics, optics, and light-emitting diodes," *Materials Today Nano,* vol. 6, p. 100036, 2019/06/01/ 2019, doi: https://doi.org/10.1016/j.mtnano.2019.100036.

[3] K. Lin, J. Xing, L. N. Quan *et al.*, "Perovskite light-emitting diodes with external quantum efficiency exceeding 20 per cent," *Nature,* vol. 562, no. 7726, pp. 245-248, 2018/10/01 2018, doi: 10.1038/s41586-018-0575-3.

[4] S. Lee, D. B. Kim, J. C. Yu *et al.*, "Versatile Defect Passivation Methods for Metal Halide Perovskite Materials and their Application to Light-Emitting Devices," *Advanced Materials,* vol. 31, no. 20, p. 1805244, 2019, doi: 10.1002/adma.201805244.

[5] S. Colella, M. Mazzeo, A. Rizzo *et al*, "The Bright Side of Perovskites," *The Journal of Physical Chemistry Letters,* vol. 7, no. 21, pp. 4322-4334, 2016/11/03 2016, doi: 10.1021/acs.jpclett.6b01799.

[6] T. Zhao, C.-C. Chueh, Q. Chen *et al*, "Defect Passivation of Organic–Inorganic Hybrid Perovskites by Diammonium Iodide toward High-Performance Photovoltaic Devices," *ACS Energy Letters,* vol. 1, no. 4, pp. 757-763, 2016/10/14 2016, doi: 10.1021/acsenergylett.6b00327.

[7] X. Y. Chin, A. Perumal, A. Bruno *et al.*, "Self-assembled hierarchical nanostructured perovskites enable highly efficient LEDs via an energy cascade," *Energy & Environmental Science,* 10.1039/C8EE00293B vol. 11, no. 7, pp. 1770-1778, 2018, doi: 10.1039/C8EE00293B.

[8] L. N. Quan, Y. Zhao, F. P. G. de Arquer *et al.*, "Tailoring the Energy Landscape in Quasi-2D Halide Perovskites Enables Efficient Green-Light Emission," *Nano Letters,* vol. 17, no. 6, pp. 3701-3709, 2017/06/14 2017, doi: 10.1021/acs.nanolett.7b00976.

[9] N. Yantara, A. Bruno, A. Iqbal *et al.*, "Designing Efficient Energy Funneling Kinetics in Ruddlesden–Popper Perovskites for High-Performance Light-Emitting Diodes," *Advanced Materials,* vol. 30, no. 33, p. 1800818, 2018, doi: 10.1002/adma.201800818.

[10] Y. F. Ng, S. A. Kulkarni, S. Parida *et al.*, "Highly efficient Cs-based perovskite light-emitting diodes enabled by energy funnelling," *Chemical Communications,* 10.1039/C7CC06615E vol. 53, no. 88, pp. 12004-12007, 2017, doi: 10.1039/C7CC06615E.

[11] J. Guo, Z. Shi, J. Xia *et al.*, "Phase Tailoring of Ruddlesden–Popper Perovskite at Fixed Large Spacer Cation Ratio," *Small,* vol. n/a, no. n/a, p. 2100560, 2021, doi: https://doi.org/10.1002/smll.202100560.

[12] M. Yuan, L. N. Quan, R. Comin *et al.*, "Perovskite energy funnels for efficient light-emitting diodes," *Nat Nano,* Article vol. advance online publication, 06/27/online 2016, doi: 10.1038/nnano.2016.110
http://www.nature.com/nnano/journal/vaop/ncurrent/abs/nnano.2016.110.html#supplementary-information.

[13] M. Yu, C. Yi, N. Wang *et al.*, "Control of Barrier Width in Perovskite Multiple Quantum Wells for High Performance Green Light–Emitting Diodes," *Advanced Optical Materials,* vol. 7, no. 3, p. 1801575, 2019, doi: 10.1002/adom.201801575.

[14] Y. Jiang, C. Qin, M. Cui *et al.*, "Spectra stable blue perovskite light-emitting diodes," *Nature Communications,* vol. 10, no. 1, p. 1868, 2019/04/23 2019, doi: 10.1038/s41467-019-09794-7.

[15] T. Zhang, L. Xie, L. Chen *et al.*, "In Situ Fabrication of Highly Luminescent Bifunctional Amino Acid Crosslinked 2D/3D NH3C4H9COO(CH3NH3PbBr3)n Perovskite Films," *Advanced Functional Materials,* vol. 27, no. 1, p. 1603568, 2017, doi: 10.1002/adfm.201603568.

[16] B. Febriansyah, T. M. Koh, Y. Lekina *et al.*, "Improved Photovoltaic Efficiency and Amplified Photocurrent Generation in Mesoporous n = 1 Two-Dimensional Lead–Iodide Perovskite Solar

Cells," *Chemistry of Materials,* vol. 31, no. 3, pp. 890-898, 2019/02/12 2019, doi: 10.1021/acs.chemmater.8b04064.

[17] D. Phuyal, M. Safdari, M. Pazoki *et al.*, "Electronic Structure of Two-Dimensional Lead(II) Iodide Perovskites: An Experimental and Theoretical Study," *Chemistry of Materials,* vol. 30, no. 15, pp. 4959-4967, 2018/08/14 2018, doi: 10.1021/acs.chemmater.8b00909.

[18] L. Mao, W. Ke, L. Pedesseau *et al.*, "Hybrid Dion–Jacobson 2D Lead Iodide Perovskites," *Journal of the American Chemical Society,* vol. 140, no. 10, pp. 3775-3783, 2018/03/14 2018, doi: 10.1021/jacs.8b00542.

[19] M. E. Kamminga, G. A. de Wijs, R. W. A. Havenith *et al.*, "The Role of Connectivity on Electronic Properties of Lead Iodide Perovskite-Derived Compounds," *Inorganic Chemistry,* vol. 56, no. 14, pp. 8408-8414, 2017/07/17 2017, doi: 10.1021/acs.inorgchem.7b01096.

[20] J. L. Knutson, J. D. Martin, and D. B. Mitzi, "Tuning the Band Gap in Hybrid Tin Iodide Perovskite Semiconductors Using Structural Templating," *Inorganic Chemistry,* vol. 44, no. 13, pp. 4699-4705, 2005/06/01 2005, doi: 10.1021/ic050244q.

[21] F. Krieg, S. T. Ochsenbein, S. Yakunin *et al.*, "Colloidal CsPbX3 (X = Cl, Br, I) Nanocrystals 2.0: Zwitterionic Capping Ligands for Improved Durability and Stability," *ACS Energy Letters,* vol. 3, no. 3, pp. 641-646, 2018/03/09 2018, doi: 10.1021/acsenergylett.8b00035.

[22] Z. Ren, J. Yu, Z. Qin *et al.*, "High-Performance Blue Perovskite Light-Emitting Diodes Enabled by Efficient Energy Transfer between Coupled Quasi-2D Perovskite Layers," *Advanced Materials,* vol. 33, no. 1, p. 2005570, 2021, doi: https://doi.org/10.1002/adma.202005570.

[23] Y. Shang, Y. Liao, Q. Wei *et al.*, "Highly stable hybrid perovskite light-emitting diodes based on Dion-Jacobson structure," *Science Advances,* vol. 5, no. 8, p. eaaw8072, 2019, doi: 10.1126/sciadv.aaw8072.

[24] B. Febriansyah, Y. Lekina, B. Ghosh *et al.*, "Molecular Engineering of Pure 2D Lead-Iodide Perovskite Solar Absorbers Displaying Reduced Band Gaps and Dielectric Confinement," *ChemSusChem,* vol. 13, no. 10, pp. 2693-2701, 2020, doi: https://doi.org/10.1002/cssc.202000028.

[25] K. Pradeesh, K. N. Rao, and G. V. Prakash, "Synthesis, structural, thermal and optical studies of inorganic-organic hybrid semiconductors, R-PbI4," *Journal of Applied Physics,* vol. 113, no. 8, p. 083523, 2013, doi: 10.1063/1.4792667.

[26] E. R. Dohner, E. T. Hoke, and H. I. Karunadasa, "Self-Assembly of Broadband White-Light Emitters," *Journal of the American Chemical Society,* vol. 136, no. 5, pp. 1718-1721, 2014/02/05 2014, doi: 10.1021/ja411045r.

[27] L. Mao, Y. Wu, C. C. Stoumpos *et al.*, "White-Light Emission and Structural Distortion in New Corrugated Two-Dimensional Lead Bromide Perovskites," *Journal of the American Chemical Society,* vol. 139, no. 14, pp. 5210-5215, 2017/04/12 2017, doi: 10.1021/jacs.7b01312.

[28] T. Hu, M. D. Smith, E. R. Dohner *et al.*, "Mechanism for Broadband White-Light Emission from Two-Dimensional (110) Hybrid Perovskites," *The Journal of Physical Chemistry Letters,* vol. 7, no. 12, pp. 2258-2263, 2016/06/16 2016, doi: 10.1021/acs.jpclett.6b00793.

[29] D. Cortecchia, J. Yin, A. Bruno, *et al.*. "Polaron Self-localization in white-light emitting hybrid perovskites." https://arxiv.org/abs/1603.01284v2 (accessed August 8, 2019.

[30] D. Cortecchia, S. Neutzner, A. R. S. Kandada *et al.*, "Broadband Emission in Two-Dimensional Hybrid Perovskites: The Role of Structural Deformation," *Journal of the American Chemical Society,* vol. 139, no. 1, pp. 39-42, 2017/01/11 2017, doi: 10.1021/jacs.6b10390.

[31] B. Saparov and D. B. Mitzi, "Organic–Inorganic Perovskites: Structural Versatility for Functional Materials Design," *Chemical Reviews,* vol. 116, no. 7, pp. 4558-4596, 2016/04/13 2016, doi: 10.1021/acs.chemrev.5b00715.

[32] M. W. Lufaso and P. M. Woodward, "Jahn-Teller distortions, cation ordering and octahedral tilting in perovskites," *Acta Crystallographica Section B,* vol. 60, no. 1, pp. 10-20, 2004, doi: doi:10.1107/S0108768103026661.

[33] K. Robinson, G. V. Gibbs, and P. H. Ribbe, "Quadratic Elongation: A Quantitative Measure of Distortion in Coordination Polyhedra," *Science,* vol. 172, no. 3983, p. 567, 1971, doi: 10.1126/science.172.3983.567.

[34] B. Febriansyah, T. Borzda, D. Cortecchia *et al.*, "Metal Coordination Sphere Deformation Induced Highly Stokes-Shifted, Ultra Broadband Emission in 2D Hybrid Lead-Bromide Perovskites and Investigation of Its Origin," *Angewandte Chemie International Edition,* vol. 59, no. 27, pp. 10791-10796, 2020, doi: https://doi.org/10.1002/anie.201915708.

[35] N. Wang, L. Cheng, R. Ge *et al.*, "Perovskite light-emitting diodes based on solution-processed self-organized multiple quantum wells," *Nat Photon,* Letter vol. 10, no. 11, pp. 699-704, 11//print 2016, doi: 10.1038/nphoton.2016.185 http://www.nature.com/nphoton/journal/v10/n11/abs/nphoton.2016.185.html#supplementary-information.

[36] X. Yang, X. Zhang, J. Deng *et al.*, "Efficient green light-emitting diodes based on quasi-two-dimensional composition and phase engineered perovskite with surface passivation," *Nature Communications,* vol. 9, no. 1, p. 570, 2018/02/08 2018, doi: 10.1038/s41467-018-02978-7.

[37] Z. Fang, W. Chen, Y. Shi *et al.*, "Dual Passivation of Perovskite Defects for Light-Emitting Diodes with External Quantum Efficiency Exceeding 20%," *Advanced Functional Materials,* vol. 30, no. 12, p. 1909754, 2020, doi: https://doi.org/10.1002/adfm.201909754.

[38] Y. F. Ng, B. Febriansyah, N. F. Jamaludin *et al.*, "Design of 2D Templating Molecules for Mixed-Dimensional Perovskite Light-Emitting Diodes," *Chemistry of Materials,* vol. 32, no. 19, pp. 8097-8105, 2020/10/13 2020, doi: 10.1021/acs.chemmater.0c00513.